Probing QGP Properties at The sPHENIX Experiment

Weihu Ma for the sPHENIX Collaboration
Institute of Modern Physics and Key Laboratory of Nuclear Physics and Ion-beam Application, Fudan University, Shanghai 200433, People's Republic of China
E-mail: maweihu@fudan.edu.cn

August 2023

Abstract. sPHENIX stands as a state-of-the-art experiment at the Relativistic Heavy Ion Collider, with its primary scientific objectives centering on probing the strongly interacting Quark-Gluon Plasma. This is achieved through high-precision measurements of hard probes within $p + p$, p+Au, and Au+Au collisions. Notably, sPHENIX can provide measurements in the low transverse momentum region and offer kinematic overlap with the experiments at the Large Hadron Collider. The scientific pursuits of sPHENIX encompass a quartet of central themes: jet and photon physics, upsilon spectroscopy, open heavy flavor, and the realm of cold quantum chromodynamics. This proceeding elucidates the experiment's overarching scientific mission, expounds upon its ingeniously crafted detector design, and delineates the paramount performance criteria that underpin its operation. Conclusively, a glimpse into the anticipated outcomes of select measurements is also proffered for consideration.

1. Introduction

The Quark-Gluon Plasma (QGP) [1] represents a new form of matter characterized by remarkably low viscosity. It dominated the early universe for the initial six microseconds following the occurrence of the big bang. The outcomes derived from the Relativistic Heavy Ion Collider (RHIC) [2] and the Large Hadron Collider (LHC) [3] have unveiled the presence of QGP, achievable through collisions of relativistic heavy ions. The experimental scrutiny of QGP serves as a direct avenue for illuminating fundamental scientific inquiries, including those concerning the phase structure of Quantum Chromodynamics (QCD) and the restoration of chiral symmetry. The investigation of QGP necessitates precise measurements of hard probes encompassing jets, upsilon particles, and various other probes within the energy regime of RHIC.

The sPHENIX experiment will provide crucial insights into understanding the inner workings of the QGP through measurements of hard probes at RHIC [4]. It was proposed that sPHENIX would serve as an upgrade and replacement for the PHENIX experiment in 2010. In the subsequent years, detailed physics cases and detector designs have been successively developed [5, 6]. The sPHENIX collaboration was established in early 2016, comprising more than 360 members from 82 institutions across 14 countries by 2022. The installation of the detectors was completed and the first run started in March 2023.

Table 1: Summary of the sPHENIX Beam Use Proposal for years 2023 - 2025. The values in parentheses correspond to the 28-cryo-week scenario.

Year	Species	$\sqrt{s_{NN}}$ [GeV]	Cryo Weeks	Physics Weeks	Rec. Lum. $\|z\| < 10$ cm	Samp. Lum. $\|z\| < 10$ cm
2023	Au+Au	200	24(28)	9(13)	3.7(5.7) nb^{-1}	4.5(6.9) nb^{-1}
2024	$p^{\uparrow}p^{\uparrow}$	200	24(28)	12(16)	0.3(0.4)pb^{-1}[5kHz] 4.5(6.2)pb^{-1}[10%-str]	45(62)pb^{-1}
2024	$p^{\uparrow}$+Au	200	-	5	0.003pb^{-1}[5kHz] 0.01pb^{-1}[10%-str]	0.11pb^{-1}
2025	Au+Au	200	24(28)	20.5(24.5)	13(15)nb^{-1}	21(25)nb^{-1}

Further information regarding the status and performance of the sPHENIX experiment can be found in the earlier proceedings published in EPJ Web of Conference, which were prepared by Hideki Okawa for the 20th International Conference on Strangeness in Quark Matter (SQM 2022) [7].

2. sPHENIX Physics

The sPHENIX experiment is a specific priority outlined in the DOE/NSF NSAC 2015 Nuclear Physics Long Range Plan. It is anticipated that this endeavor can be accomplished within three years of operation, during which it will conduct unparalleled and precise measurements of high-energy probes of the QGP at RHIC. These measurements aim to investigate the physical origin and evolution of the QGP, its internal structure, its dependence on initial temperature, and its interactions with various high-energy probes. A summary of the sPHENIX Beam Use Proposal for the years 2023-2025 is provided in Table 1 [8].

Commencing from March 2023, over 50% of the Year-1 data is allocated for the commissioning of all detector subsystems and full detector operations. This phase will also serve to validate calibration and reconstruction processes. During the inaugural year of the run plan, the collection of Au+Au data sets will be initiated, enabling sPHENIX to replicate and expand upon "standard candle" measurements at RHIC. In Year-2 (2024), the detector commissioning will extend to $p + p$ collisions, yielding extensive datasets essential as references for heavy ion physics. Additionally, a sizable p+Au data set will be collected, introducing new opportunities for studying cold QCD. Year-3 (2025) will concentrate on accumulating a substantially extensive dataset of Au+Au collisions, providing unparalleled statistical precision and accurate measurements of jets and heavy flavor observables.

The four core physics programs of sPHENIX encompass jet and photon physics across a range of momentum and angular scales, upsilon spectroscopy involving various sizes, open heavy flavor studies spanning different momentum scales and parton masses, and investigations into cold Quantum Chromodynamics designed to explore proton spin, transverse momentum, and cold nuclear effects.

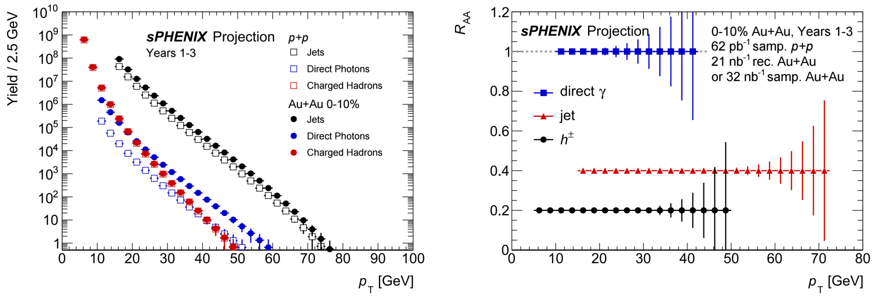

Figure 1: (color online) Projected total yields (left) and the nuclear modification factor R_{AA} (right) for jets, photons, and charged hadrons in 0 - 10% $Au + Au$ events and $p + p$ events, for the first three years of sPHENIX data-taking.

2.1. High-p_T Probes

The detection of QGP through precise measurements of jets, direct photons, and hadrons constitutes a core component of the sPHENIX scientific program. Figure 1 illustrates the projected total yields (left) and the nuclear modification factor R_{AA} (right) for jets, photons, and charged hadrons in 0-10% Au+Au events (based on a Glauber MC simulation [9]) as well as $p + p$ events, spanning the first three years of sPHENIX data collection. The combination of high data rates and a hermetic EMCal+HCal calorimeter system provides an extensive p_T range, reaching approximately 50 GeV for hadrons, 40 GeV for photons, and 70 GeV for jets. Notably, sPHENIX excels in the precise measurement of the low p_T region, a task that proves challenging at the LHC. Furthermore, sPHENIX's kinematic range exhibits overlap with that of the LHC, thereby affording valuable opportunities for complementary investigations of hard probes under distinct QGP conditions.

2.2. Jet Physics

Over the course of the three-year data collection period, sPHENIX will collect a substantial quantity of data samples aimed at meticulously reconstructing jet measurements. These encompass various aspects such as jet yield, di-jet events, jet (sub-) structure and properties, photon-tagged jet quenching measurements, jet-hadron correlations, as well as the yield and properties of b-quark jets. In Figure 2 (left), statistical projections illustrate the jet-to-photon p_T balance $x_{J\gamma}$ for photons with $p_T >$ 30 GeV. This constitutes a "flagship" measurement characterized by high statistics and offering a direct assessment of jet energy loss. The sPHENIX measurement of $x_{J\gamma}$ presents a distinctive opportunity for comparison with the LHC, despite the significantly divergent center-of-mass energies [10]. Figure 2 (right) portrays the statistical projections of the groomed momentum fraction for jets with $p_T >$ 40 GeV. This specific projection pertains to jet substructure measurements, facilitated by sPHENIX's finely segmented calorimeter and excellent tracking resolution. The exploration of jet substructure is poised to elucidate the development of parton showers within the QGP, offering insights into fundamental parton-level splittings.

sPHENIX data will impose stringent constraints on the coupling of b-quarks to the QGP through R_{AA} measurements extending to the low-p_T region, as depicted in

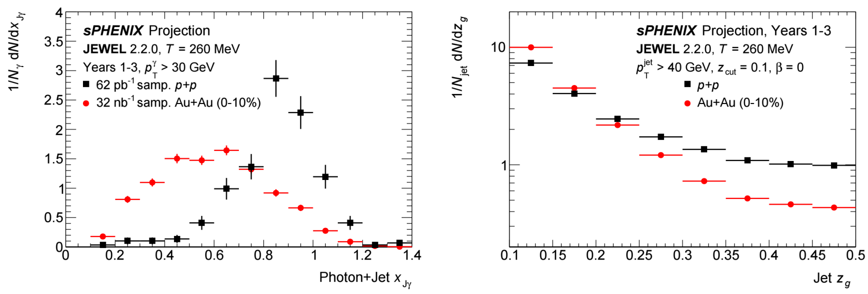

Figure 2: (color online) Statistical projections for the jet-to-photon p_T balance, $x_{J\gamma} = \frac{p_T^{jet}}{p_T^{\gamma}}$ (left) and the groomed momentum fraction $z_g = \frac{min(p_{\perp,1}, p_{\perp,2})}{p_{\perp,1}+p_{\perp,2}}$ (right).

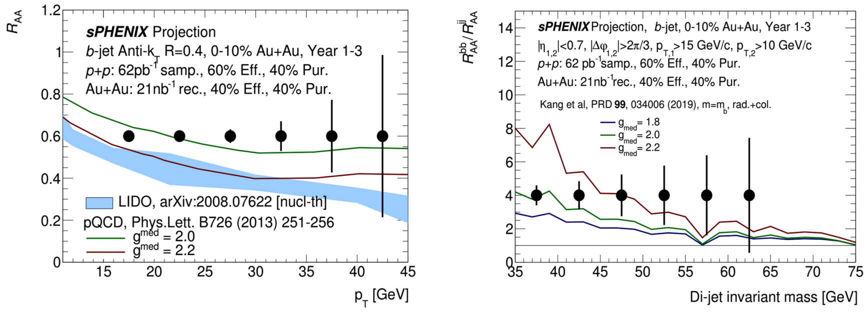

Figure 3: (color online) Projected statistical uncertainties of nuclear modification factor R_{AA} measurements of b-jets (left) as a function of p_T in 0 – 10% central Au+Au collisions at $\sqrt{s_{NN}}$ = 200 GeV from the three-year sPHENIX operation and b-jet-light-jet super-ratio (right) along with pQCD calculations from Ref. [11].

Figure 3 (left). This endeavor will mark the inaugural b-jet tagging at RHIC, founded upon sPHENIX's precision assessment of the distance of closest approach (DCA) for tracks and its secondary vertex tagger. Figure 3 (right) presents the envisaged statistical uncertainties pertaining to the suppression of back-to-back heavy-flavor di-b-jet pairs, juxtaposed with pQCD calculations. This projection underscores how the measurement of the b-jet-light-jet super-ratio will deliver strong sensitivity to the parton mass effect, thereby presenting a unique opportunity for scrutinizing the behavior of quarks within the QGP.

2.3. Open Heavy Flavor

Heavy flavor quarks traversing the QGP serve as unique probes for investigating the interaction between quarks and the QGP, encompassing mass-dependent energy loss and collectivity within the QGP medium. Leveraging sPHENIX's state-of-the-art vertex tracking system and high-rate streaming DAQ, precision measurements of heavy flavor at RHIC will subject models describing the coupling between heavy quarks and the QGP medium to rigorous scrutiny.

Benefiting from the distinct separation of open bottom quarks through Distance of DCA analysis, sPHENIX will conduct a comparative analysis of non-prompt and prompt D^0 mesons. Figure 4 (left) showcases the projected R_{AA} measurements for non-prompt/prompt D^0 mesons, revealing that nuclear modifications for bottom quarks and

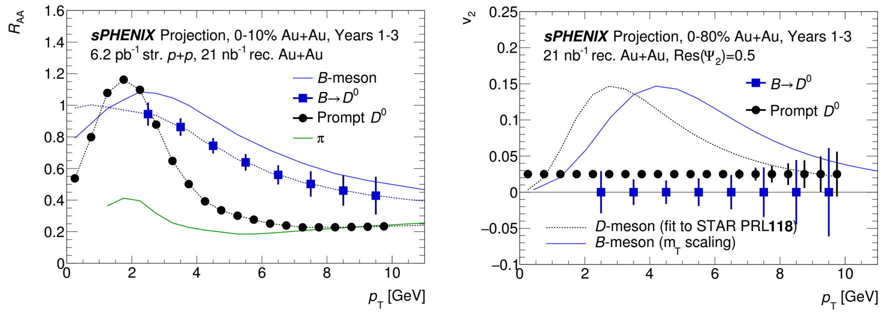

Figure 4: (color online) Projected statistical uncertainties of R_{AA} (left) and v_2 (right) measurements of non-prompt/prompt D^0 mesons.

light quarks are anticipated to exhibit marked differences for $p_T < 15$ GeV. Figure 4 (right) offers a projection of elliptic flow v_2 measurements for non-prompt/prompt D^0 mesons within the low-p_T range. These measurements, achieved with unprecedented precision, promise a distinctive perspective on the interaction between heavy flavor quarks and the medium. Furthermore, they will exert substantial constraints on the heavy quark diffusion transport parameter of the QGP medium, including its temperature dependence.

sPHENIX's capabilities extend to the precise measurement of the Λ_c/D ratio at RHIC, contributing to an enhanced understanding of charm hadronization.

2.4. Upsilon Spectroscopy

The Upsilon particle arises from hard scatterings in the early stages of relativistic heavy-ion collisions, consequently traversing the entire evolution of the QGP. The sPHENIX experiment uniquely stands poised to explore the distinct suppression effects exerted by the QGP medium on the three quantum states of the Upsilon particle via di-electron channels. This distinctive capability capitalizes on sPHENIX's exceptional precision in measuring Upsilon production, underscored by its remarkable mass resolution of δM $<$ 125 MeV and robust signal extraction prowess. This enables the clear differentiation of the $\Upsilon(1S, 2S, 3S)$ states. The investigation of centrality and, in particular, the p_T dependence holds pivotal importance for fostering comparisons between RHIC and the LHC (Figure 5).

Leveraging machine learning offers substantial advantages in particle identification. The machine learning algorithm developed by the sPHENIX simulation group is anticipated to significantly enhance the identification accuracy of signal electrons, bolster the rejection efficiency for background hadrons, and consequently amplify the signal-to-noise ratio for Upsilon particle measurements. This advancement is especially noteworthy for the signal extraction of the 3^{rd} state, which was recently observed for the first time in Pb+Pb collisions by CMS [12].

2.5. Cold QCD

Equipped with trigger capabilities and a high-rate DAQ system, sPHENIX also presents invaluable opportunities for delving into cold QCD investigations through the measurements of jets, photons, and charged hadrons in $p+p$ and p+Au collisions. Figure

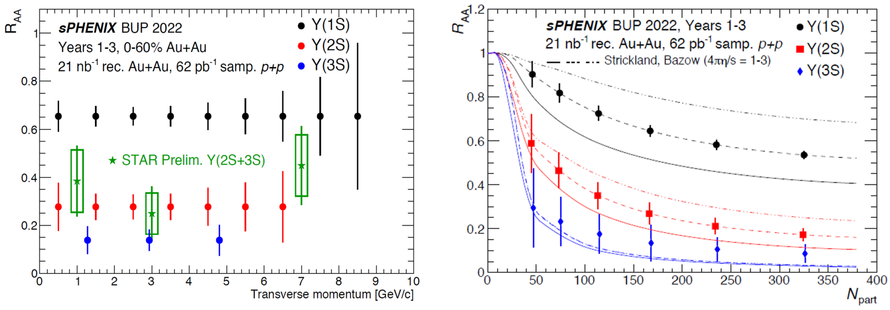

Figure 5: (color online) Projected statistical uncertainties of R_{AA} measurements of Upsilon three states relative to p_T (left) and N_{part}.

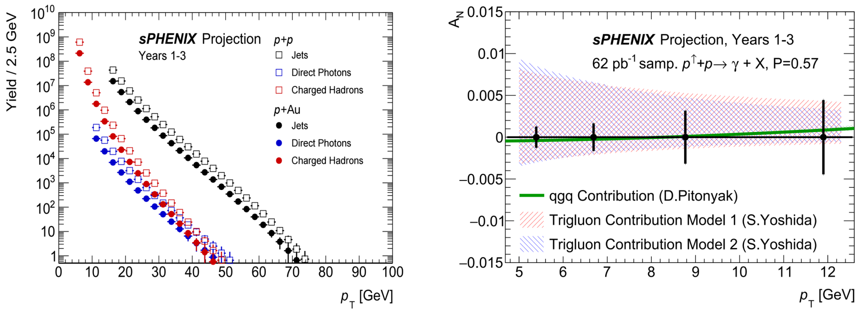

Figure 6: (color online) Projected total yields (left) for jets, photons, and charged hadrons in centrality-integrated $p + p$ and $p + Au$ events, and projected statistical uncertainties for direct photon the transverse spin asymmetry A_N (right), for the first three years of sPHENIX data-taking.

6 (left) illustrates the anticipated total yields for jets, photons, and charged hadrons in centrality-integrated $p + p$ and p+Au events. This projection suggests that sPHENIX is poised to amass ample data, facilitating jet measurements reaching up to approximately 70 GeV, and capturing charged hadrons and photons up to approximately 45 GeV. Spin-related measurements at sPHENIX, including the transverse single spin asymmetry (TSSA), can be realized through prompt photons and D_0 mesons in beam-polarized $p^{\uparrow}+p$ collisions. This setup serves as a probe to explore gluon dynamics within a transversely polarized nucleon, incorporating tri-gluon correlations. Figure 6 (right) outlines the envisaged statistical uncertainties for the direct photon transverse spin asymmetry A_N.

3. sPHENIX Detector

The sPHENIX detector stands out due to its high data rates of 15 kHz for all subdetectors, coupled with extensive coverage and precise tracking and calorimetry systems. Its focus lies in introducing new measurement capabilities within the RHIC energy range. This encompasses enabling comprehensive, unbiased jet reconstruction, b-jet tagging, and investigations into the three upsilon states, both in heavy-ion and pp collisions. The sPHENIX detector's configuration is depicted in Figure 7 and comprises a tracking system and a calorimetry system. The tracking system is comprised of the MAPS-based micro-vertex detector (MVTX), the intermediate tracking detector (INTT), the time projection chamber (TPC), and the TPC outer tracker (TPOT), ordered from

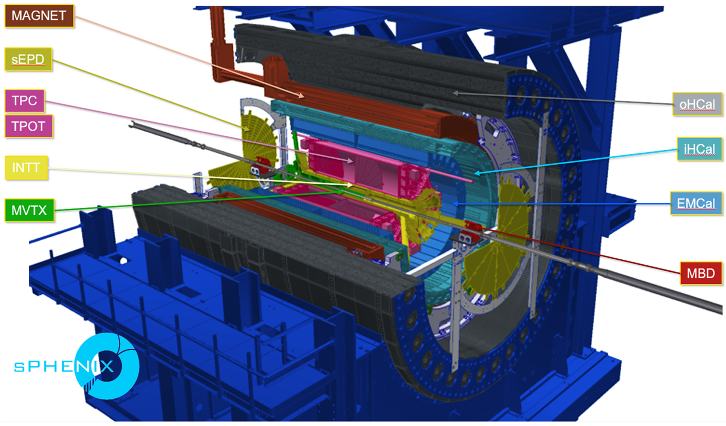

Figure 7: (color online) The engineering drawing of the sPHENIX detector with its support structure.

the innermost to the outermost layer. This tracking system is enveloped by a calorimeter situated within a 1.5 Tesla Solenoid magnet. The calorimeter design encompasses an electromagnetic calorimeter (EMCal) and two hadron calorimeters (HCal): the inner HCal (iHCAL) and the outer HCal (oHCal). The iHCal is positioned within the Solenoid magnet, while the oHCal is located outside it. Additionally, flanking the collision point along the beam axis are the minimum bias detector (MBD) and the sPHENIX event plane detectors (sEPD). The sPHENIX detector provides complete azimuthal (φ) coverage of 4π and covers a pseudo-rapidity (η) range from -1.1 to 1.1. Its hybrid streaming/triggered readout system enables optimal utilization of the RHIC's luminosity.

3.1. Tracking Detectors:MVTX, INTT, TPC, and TPOT

The MVTX, positioned in close proximity to the beam pipe, incorporates 3-layer Monolithic Active Pixel Sensors (MAPS) technology. This design draws inspiration from the ALICE ITS-2 inner barrel design (ITS-2) [13], and it excels in achieving an excellent 2-D DCA resolution. This capability is crucial for delivering highly precise vertex measurements, particularly for decays of particles containing b and c quarks. The INTT, comprised of two barrels with two layers each, utilizes silicon strip detectors. These components are placed within the TPC. Notably, the INTT has a fast O(100 ns) integration time, enabling it to effectively resolve one beam crossing. Encompassing pseudorapidities $\eta < |1.1|$, the TPC represents a compact structure equipped with 48 layers, with radii ranging from 20 to 78 cm. This implementation is based on the Gas Electron Multiplier technology, which plays a crucial role in providing sPHENIX with the requisite invariant mass resolution [14]. Inserted between the TPC and EMCal, the TPOT is composed of 8 Micromegas modules. It serves the critical purpose of calibrating beam-induced space charge distortions within the TPC, ensuring the accuracy of measurements.

With an efficiency of approximately 90% for $p+p$ collisions at $p_T > 1$ GeV (depicted in Figure 8, left panel), this tracking system holds great promise for investigating rare processes, such as $\Upsilon(nS)$ decays. Furthermore, the tracking p_T resolution is maintained at less than 2% for $p_T < 10$ GeV (as illustrated in Figure 8, middle panel), thereby satisfying the requirement of achieving δM < 125 MeV for the separation of $\Upsilon(nS)$ states. Equally

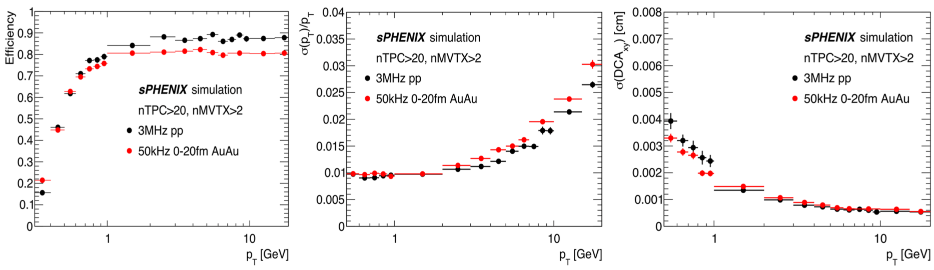

Figure 8: (color online) Tracking performance for reconstruction efficiency (left), the p_T resolution (middle), and the DCA resolution in the transverse direction (xy) (right) as a function of track p_T.

crucial is the system's ability to achieve excellent DCA resolutions in both $r - \Phi$ and z dimensions, with values remaining below 40 μm for $p_T > 0.5$ GeV (as demonstrated in Figure 8, right panel). This level of precision is of paramount importance for conducting accurate open heavy-flavor measurements.

3.2. Calorimeters:EMCal, inner-HCal, and outer-HCal

The calorimetry system consisting of EMCal, iHCal, and oHCal has a compact structure with coverage of $|\eta| < 1.1$ and 2π in φ and with a common light collection followed by silicon photomultipliers (SiPM) readout for both EMCal and HCal. The EMCal is built with a granular segmentation of $\Delta\eta \times \Delta\varphi = 0.025 \times 0.025$, utilizing a Tungsten/scintillating fiber SPACAL. It has a small Moliere radius, a short radiation length, and an impressive energy resolution of $\sigma_E/E \leq 16\%/\sqrt{E}$ [15, 16]. This configuration enables efficient electron identification for the Υ and photon measurements. Additionally, it serves as a crucial component for jet reconstruction, working in tandem with the iHCal and oHCal. The iHCal is constructed using aluminum-scintillating tiles embedded with wavelength shifting (WLS) fibers, while the oHCal is assembled using tilted steel plates and scintillator tiles with embedded WLS fibers. Both the iHCal and oHCal are subdivided into granular towers with dimensions of $\Delta\eta \times \Delta\varphi = 0.1 \times 0.1$. The overall HCal achieves an energy resolution of approximately $20\%/\sqrt{E}$ [15], a performance level that satisfies the jet energy resolution requirement.

3.3. Minimum Bias Detector

The sPHENIX MBD delivers a high-efficiency minimum-bias trigger, surpassing 90% efficiency for heavy ion collisions. It plays a crucial role in various aspects, including the reconstruction of centrality, reaction plane, start time, and interaction vertex. The MBD is ingeniously repurposed from the existing PHENIX Beam-Beam counter, incorporating 2×64 channels of 3 cm thick quartz radiator aligned with a mesh dynode photomultiplier. Notably, it achieves a remarkable timing resolution of 120 ps.

3.4. sPHENIX Event Plane Detector

The sEPD is for measuring the event plane and centrality outside of mid-rapidity, covering a range of $2.0 < |\eta| < 4.9$. Its exploits 1.2-cm-thick scintillators with WLS fibers and consists of two wheels of 12 sectors with 31 optically-isolated tiles.

3.5. Hybrid Data Acquisition Structure

sPHENIX adopts a hybrid DAQ of two paths for data taking. One is the nominal sPHENIX DAQ model assuming calorimeter-based Level-1 triggers for the observables, such as photons and jets, leave clear signatures in the calorimeter system. The other one is the streaming readout mode supported by all tracking detectors s (MVTX, INTT, and TPC) without requiring the Level-1 trigger and it's for recording 10% of all collisions. This hybrid trigger-streaming DAQ will significantly increase $p + p$ data collection and is crucial for open heavy flavor physics as well as cold QCD measurements.

4. Conclusions

With high DAQ and trigger rate, sPHENIX enables new measurements of the microscopic nature of QGP. It is a state-of-the-art experiment at RHIC and consists of a highly precise tracking system and a large-hermetic calorimetry system, providing unique opportunities in low energy and offering kinematic overlap with the LHC. A wide range of physics are covered at sPHENIX: jet and photon physics, upsilon spectroscopy, open heavy flavor, and cold QCD. The installation of the detectors was completed, with the first data acquisition scheduled for 2023.

5. References

[1] W. Busza, K. Rajagopal, W. van der Schee, Ann. Rev. Nucl. Part. Sci. 68, 339 (2018)
[2] A. Adare et al., Phys. Rev. Lett., 104:132301, (2010).
[3] M. Luzum and P. Romatschke, Phys. Rev. Lett., 103:262302, (2009).
[4] A. Aprahamian et al., Reaching the horizon: The 2015 long range plan for nuclear science (2015).
[5] A. Adare et al., sPHENIX Note, Science Proposal (2014), arXiv:1501.06197.
[6] sPHENIX Collaboration, sPHENIX Technical Design Report (2019), https://indico.bnl.gov/event/7081.
[7] Hideki Okawa for the sPHENIX Collaboration, EPJ Web of Conferences 276, 05004 (2023).
[8] sPHENIX Collaboration, sPHENIX Beam Use Proposal, sPH-TRG-2022-001 (2022), https://indico.bnl.gov/event/15845.
[9] M. L. Miller, K. Reygers, S. J. Sanders, and P. Steinberg. Glauber modeling in high energy nuclear collisions. Ann. Rev. Nucl. Part. Sci., 57:205 – 243, 2007. doi:10.1146/annurev.nucl.57.090506.123020. 7.1
[10] W. Dai, I. Vitev, B. W. Zhang, Phys. Rev. Lett. 110, 142001 (2013).
[11] Zhong-Bo Kang, Jared Reiten, Ivan Vitev, and Boram Yoon. Light and heavy flavor dijet production and dijet mass modification in heavy ion collisions. Phys. Rev. D, 99(3):034006, 2019. arXiv:1810.10007, doi:10.1103/PhysRevD.99.034006. 7.7, 7.3
[12] CMS Collaboration, CMS Note, CMS-PAS-HIN-21-007 (2022).
[13] ALICE Collaboration, J. Phys. G: Nucl. Part. Phys. 41, 087002 (2014).
[14] H Klest, J. Phys.: Conf. Ser. 1498 012025 (2020).
[15] C.A. Aidala et al., IEEE Trans. Nucl. Sci. 65, 2901 (2018).
[16] C.A. Aidala et al., IEEE Trans. Nucl. Sci. 68, 173 (2021).